Electronic Supplementary Material (ESI) for ChemComm.

Electronic Supporting Information

Long-Range Ferromagnetism in Nickel Based Hybrid Structure with Semiconductor Behavior

Prabu Mani,[a] Arkamita Bandyopadhyay,[b] Prashanta K. Mukharjee,[c] Ramesh Chandra Nath,[c] Swapan K. Pati[b] and Sukhendu Mandal[a]*

[a]School of Chemistry, Indian Institute of Science Education and Research Thiruvananthapuram, Thiruvananthapuram, Kerala, India-695551.

[b]Theoretical Chemistry Unit and New Chemistry Unit, Jawaharlal Nehru Centre for Advanced Scientific Research, Bangalore, India-560064.

[c]School of Physics, Indian Institute of Science Education and Research Thiruvananthapuram, Thiruvananthapuram, Kerala, India-695551.

Materials and Methods:

All chemicals were of reagent-grade quality and used without further purification. Nickel (II) chloride was purchased from TCI chemicals, whereas 1,3,5-Tris(4-carboxyphenyl)benzene (BTB) and 1,2-bis (4-pyridyl) ethane (BPE) were purchased from Sigma-Aldrich. N, N'-dimethylformamide [DMF] and milli-Q water as solvents used for synthesis.

The single crystal diffraction data were collected using Bruker AXS Smart Apex CCD diffractometer at 150 K. The data were reduced using SAINTPLUS[1] and an empirical absorption correction was applied using the SADABS program.[2] Crystal structure was solved by direct methods using SHELXS2018 and refined using SHELXL2018 present in the SHELXTL V6.14.[3] Full-matrix-least-squares structure refinement against F^2 was carried out using the WINGX[4] package of programs. Powder X-ray diffraction data were collected using an X'pert PRO (PANalytics) powder diffractometer equipped with Cu K_α radiation (1.5405 Å). IR spectra were recorded from prepared KBr pellets, using IR prestige-21 (Shimadzu) spectrometer. The TGA was performed on SDT Q600 (Shimadzu) analyzer, gas sorption measurements were carried out on a Micromeritics 3Flex gas sorption analyzer. EPR analysis were carried out using Bruker Ems EPR spectrometer, frequency is 9.43 GHz, 2,2-diphenyl-1-picrylhydrazyl (DPPH) used as reference.

Synthetic procedure for compound 1:

$NiCl_2$ (0.20 mmol), 1,3,5-Tris(4-carboxyphenyl)benzene (BTB) (0.05 mmol) and 1,2-bis (4-pyridyl) ethane (0.10 mmol) were dissolved in 10 mL of solvent mixture (7 mL DMF + 3 mL milli-Q water). This solution was sonicated for 5 min then transferred into a Parr Teflon-lined vessel (23 mL). Then vessel was sealed in an autoclave and heated at 100 ^{0}C for 3 days in a programmable oven. This reaction yield cyano-colored needle shaped crystals (compound **1**).

Sample preparation for magnetic measurement:

The as-synthesized compound **1 (**crystals) were washed thrice using 15 mL of Milli-Q water then the sample was placed under vacuum about 12 h at room temperature for drying. The dried sample was well ground using mortar and pestle. The powder sample was packed in a Teflon sample holder which was then attached to the vibrating sample magnetometer (VSM) sample rod. The whole assembly was inserted inside the VSM attachment to the PPMS for measurements.

Optical Band-Gap Measurements

The optical absorption spectra of **1** was collected on a Shimadzu UV/Vis/NIR spectrophotometer. The room temperature diffuse reflectance spectra was measured using $BaSO_4$ as a reference material and converted to a Kubelka–Munk function, from which the band gap of the compound was estimated.[5] This two-flux model, which considers only diffuse light, is used to determine the absorption coefficient from a surface that both scatters and absorbs incident radiation. For a crystalline solid with a band gap (E_{bg}), the frequency dependence (ν) of the absorption coefficient (***κ***) can be approximated as

$$\kappa(\upsilon) = \frac{B_T(h\nu - E_{bg})^n}{h\nu} \text{ ---------- (1)}$$

where B_T is a constant derived from the square of the averaged dipolar momentum matrix element and n is equal to 0.5 and 2 for direct and indirect band gap transitions, respectively.[5] The absorption coefficient (κ) can be measured from the reflectance (R) and expressed as $\kappa = (1 - R)^2/(2R)$. Using the above equation, the band gap of a material can be obtained by extrapolating to zero with the linear fit to a plot of $(kh\nu)^{1/n}$ *vs* hν.

Variable temperature electrical resistance measurement:

Variable temperature Electrical resistance was measured using Keithley 6517B electrometer with Linkam temperature controller. Approximately 100 mg compound **1** was gently ground using mortar and pestle then pelletized (0.6 mm thickness at 7-Ton pressure for 5 min). To make contacts, either side of the pellet were coated with the silver paint. Then the pellet placed in between the metal disks. Linkam temperature controller was used for temperature dependent resistance measurements (3 cm distance between leads, 5V sourced and 1 ºC/min ramp).

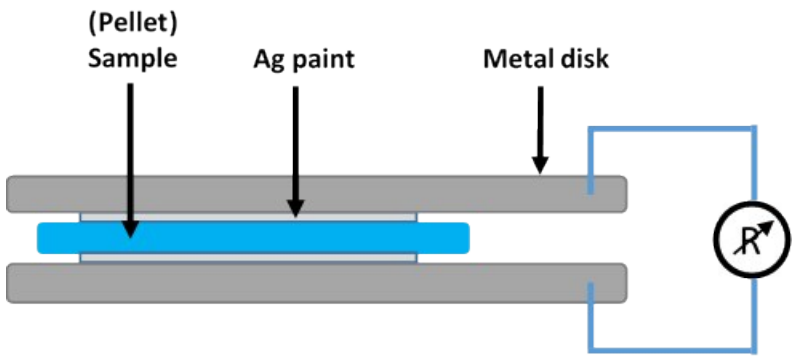

Theoretical Studies of Band Structure Calculations:

To gain insight into the observed electronic structure calculations on the periodic solids were carried out using the Vienna Ab initio Simulation Package (VASP) code.[6,7] The atomic structures were derived from the experimental X-ray diffraction data, and then the crystal structure was corrected using the identity of the reactants. A plane wave basis with an energy cutoff of 400 eV was used.[7] We used only the gamma point due to the large size of the unit cells, and for exchange and correlation functional, we used a generalized gradient approximation (GGA) functional as proposed by Perdew, Burke, and Ernzerhof (PBE).[8] The theoretical studies on the linker molecules were carried out using ADF.[9] The TZ2P basis was used with a small core.

Computational Methods:

The magnetic calculations were performed using spin polarized density functional theory (DFT) method as implemented in the SIESTA package.[10] Generalized gradient approximation (GGA) in the Perdew–Burke–Ernzerhof (PBE) form[11] has been considered to take the exchange–correlation interactions into account. We have used double-zeta-polarized (DZP) numerical atomic-orbital basis sets and norm-conserving pseudo-potentials[12] in the fully nonlocal Kleinman–Bylander form for all the atoms.[13] We have used a mesh cut-off value of 400 Ry. 20 Å vacuum has been used in all three directions to avoid any spurious interactions.

For Optical properties, we have used TD-DFT methods as implemented in Gaussian 09 package.[14] We have used the CAM-B3LYP functional which is the long-range corrected version of B3LYP[15] and employs the Coulomb-attenuating method. We have used the 6-31+g (d) basis set for all the atoms except Ni, for which we used LANL2DZ pseudo potential based approach. We have considered 12 lowest lying excited states for all the calculations.

References

1. SMART (V 5.628), SAINT (V 6.45a), XPREP, SHELXTL; Bruker AXS Inc.: Madison, WI, **2004**.
2. G. M. Sheldrick, Siemens Area Correction Absorption Correction Program; University of Göttingen: Göttingen, Germany, **1994**.
3. G. M. Sheldrick, SHELXL-97 Program for Crystal Structure Solution and Refinement; University of Göttingen: Göttingen, Germany, **1997**.
4. J. L. Farrugia, *J. App. Crystallography*. **1999**, *32*, 837-838.

5. N. Laidani, R. Bartali, G. Gottardi, M. Anderle, P. Cheyssac, *J. Phys. Condens. Matter* 2008, 20, 015216.
6. G. Kresse and J. Furthmüller, *Phys. Rev. B* **1996**, *54*, 11169.
7. G. Kresse and D. Joubert, *Phys. Rev. B* **1999**, *59*, 1758.
8. J. P. Perdew, K. Burke, and M. Ernzerhof, *Phys. Rev. Lett.* **77**, 3865 (1996).
9. G. te Velde, F.M. Bickelhaupt, E.J. Baerends, C. Fonseca Guerra, S.J.A. van Gisbergen, J.G. Snijders, and T. Ziegler*, J. Comput. Chem.* **2001**, *22*, 931.
10. J. M. Soler, E. Artacho, J. D. Gale, A. García, J. Junquera, P. Ordejón, D. Sánchez-Portal, The SIESTA Method for Ab Initio Order-N Materials Simulation. *J. Phys.: Condens. Matter.* **2002**, *14*, 2745-2779.
11. K. Burke, J. P. Perdew, M. Ernzerhof, Why the Generalized Gradient Approximation Works and How to Go Beyond It. *Int. J. Quantum Chem.***1997**, *61*, 287-293.
12. N. Troullier, J. L. Martins, Efficient Pseudopotentials for Plane-Wave Calculations. *Phys. Rev. B: Condens. Mater.* **1991**, *43*, 1993-2006.
13. L. Kleinman, D. Bylander, Efficacious Form for Model Pseudopotentials. *Phys. Rev. Lett.* **1982**, *48*, 1425-1428.
14. M. Robb, J. R. Cheeseman, G. Scalmani, V. Barone, B. Mennucci, G. A. Petersson, H. Nakatsuji, M. Caricato, X. Li, H. P. Hratchian, A. F. Izmaylov, J. Bloino, G. Zheng, J. L. Sonnenberg, M. Hada, M. Ehara, K. Toyota, R. Fukuda, J. Hasegawa, M. Ishida, T. Nakajima, Y. Honda, O. Kitao, H. Nakai, T. Vreven, Jr. J. A. Montgomery, J. E. Peralta, F. Ogliaro, M. Bearpark, J. J. Heyd, E. Brothers, K. N. Kudin, V. N. Staroverov, R. Kobayashi, J. Normand, K. Raghavachari, A. Rendell, J. C. Burant, S. S. Iyengar, J. Tomasi, M. Cossi, N. Rega, J. M. Millam, M. Klene, J. E. Knox, J. B. Cross, V. Bakken, C. Adamo, J. Jaramillo, R. Gomperts, R. E. Stratmann, O. Yazyev, A. J. Austin, R. Cammi, C. Pomelli, J. W. Ochterski, R. L. Martin, K. Morokuma, V. G. Zakrzewski, G. A. Voth, P. Salvador, J. J. Dannenberg, S. Dapprich, A. D. Daniels, Ö. Farkas, J. B. Foresman, J. V. Ortiz, J. Cioslowski, D. J. Fox, Gaussian 09, Revision D.01; Gaussian: Wallingford, CT, USA, 2009.
15. T. Yanai, D. P. Tew, N. C. Handy, A New Hybrid Exchange−Correlation Functional Using the Coulomb-Attenuating Method (CAM-B3LYP). *Chem. Phys. Lett.* **2004**, *393*, 51−57.

Single Crystal X-ray Diffraction Analysis:

Table S1: Single crystal parameter for compound **1**

Parameters	Compound 1
Chemical formula	$Ni_{1.50}\ C_{57}\ N_6\ O_{10.5}\ H_{41}$
Formula weight	1066.02
Crystal system	Monoclinic
Space Group	$P2_1/n$
a(Å)	8.6003 (2)
b(Å)	18.6486 (5)
c(Å)	34.7689 (9)
α(°)	90
β(°)	96.7110 (10)
γ(°)	90
Volume ($Å^3$)	5538.2
Z	4
Temperature (K)	150
Calculated density (g/cm^3)	1.279
θ range (°)	2.359 to 28.324
Absorption coefficient (mm^{-1})	0.577
Reflections collected	51299
Unique reflections	13628
Goodness-of-fit	0.994
Number of parameters	689
Final R indices [I > 2sigma(I)]	R_1= 0.0695, wR_2= 0.1872

[a] $R_1 = \Sigma||F_0| - |F_c||/ \Sigma|F_0|$; $wR_2 = \{[w(F_0^2 - F_c^2)^2]/ [w(F_0^2)^2]\}^{1/2}$; $w = 1/[\sigma^2(F_0)^2 + (aP)^2 + bP]$; $P = [\max(F_0^2,0) + 2(F_c)^2]/3$; a = 0.1293 , b = 0.0000

Table S2: Selected bond lengths of compound 1:

Compound 1	Bond Length (Å)
Ni(1)-O(2)	2.056(2)
Ni(1)-O(3)	2.064(2)
Ni(1)-O(1)	2.075(2)
Ni(1)-N(3)	2.095(3)
Ni(1)-N(2)	2.101(3)
Ni(1)-N(1)	2.129(3)
Ni(2)-N(4)	2.077(3)
Ni(2)-O(5)	2.089(2)
Ni(2)-O(6)	2.105(2)
Ni(2)-N(4)#1	2.077(3)
Ni(2)-O(5)#1	2.089(2)
Ni(2)-O(6)#1	2.105(2)

Symmetry transformations used to generate equivalent atoms: #1 -x+3,-y,-z

Topos for compound 1:

##########################

1:C57 H41 N6 Ni1.50 O10.50

##########################

Topology for Ni1

Atom Ni1 links by bridge ligands and has

Common vertex with				R (A-A)	f
Ni 1	1.4551	0.2328	0.2210	(1 0 0) 8.600A	1
Ni 1	-0.5449	0.2328	0.2210	(-1 0 0) 8.600A	1
Ni 2	1.5000	0.0000	0.0000	(1 0 0) 13.220A	1
Ni 2	0.5000	1.0000	0.0000	(0 1 0) 16.266A	1
Ni 2	1.0000	-0.5000	0.5000	(1-1 0) 17.093A	1
Ni 1	-0.0449	0.2672	-0.2790	(-1 0-1) 17.426A	1
Ni 1	0.9551	0.2672	0.7210	(0 0 0) 17.426A	1

Topology for Ni2

Atom Ni2 links by bridge ligands and has

Common vertex with				R (A-A)	f
Ni 1	-0.5449	0.2328	0.2210	(-1 0 0) 13.220A	1
Ni 1	1.5449	-0.2328	-0.2210	(2 0 0) 13.220A	1
Ni 1	0.4551	-0.7672	0.2210	(0-1 0) 16.266A	1
Ni 1	0.5449	0.7672	-0.2210	(1 1 0) 16.266A	1
Ni 1	-0.0449	-0.7328	-0.2790	(-1-1-1) 17.093A	1
Ni 1	1.0449	0.7328	0.2790	(1 0 0) 17.093A	1

Structural group analysis

Structural group No 1

Structure consists of 3D framework with Ni3O14N8C102H82

Coordination sequences

Ni1:	1	2	3	4	5	6	7	8	9	10
Num	7	30	95	203	332	502	682	921	1147	1466

Cum 8 38 133 336 668 1170 1852 2773 3920 5386

Rad 14.1(4.0) 22.8(6.5) 30.8(9.1) 41.1(10.9) 52.5(12.4) 64.7(14.4) 76.1(16.5) 88.1(18.8) 99.4(21.3) 111.4(23.7)

Cmp Ni7 Ni30 Ni95 Ni203 Ni332 Ni502 Ni682 Ni921 Ni1147 Ni1466

Ni2: 1 2 3 4 5 6 7 8 9 10

Num 6 30 100 204 344 494 706 900 1188 1430

Cum 7 37 137 341 685 1179 1885 2785 3973 5403

Rad 15.5(1.8) 22.3(6.7) 29.9(9.5) 41.0(10.7) 52.8(12.0) 64.5(14.2) 76.5(16.2) 87.9(18.8) 99.9(21.0) 111.2(23.7)

Cmp Ni6 Ni30 Ni100 Ni204 Ni344 Ni494 Ni706 Ni900 Ni1188 Ni1430

TD10=5391

Vertex symbols for selected sublattice

Ni1 Point symbol: {3^2.4^5.5^5.6^8.7}

Extended point symbol: [3.3.4.4.4.4.4.6.5.6(2).6(2).6(3).5.5.5.5.6(7).6(8).6(2).7(3).6(2)]

Vertex symbol: [3.3.4.4.4.4.4.6.6(2).6(2).6(2).6(3).6(4).6(5).6(5).6(5).6(7).6(8).7(3).8(3).*]

All rings (up to 8):
[3.3.4.(4,6).4.(4,6,7(3),8).(4,8(2)).6.6(2).6(2).(6(2),7(5),8(3)).(6(3),7(2)).(6(4),8).(6(5),8).(6(5),7(4),8(2)).(6(5),7(3),8).(6(7),7).(6(8),7(7),8(2)).(7(3),8).8(3).*]

Cycle sequence

Size 3 4 5 6 7 8

Num 2 5 11 62 181 767

Ni2 Point symbol: {3^2.4^2.5^2.6^9}

Extended point symbol: [3.3.4.4.6(2).6(2).6(2).6(2).6(2).6(2).6(3).6(3).5.5.6(8)]

Vertex symbol: [3.3.4.4.6(2).6(2).6(2).6(2).6(2).6(2).6(3).6(3).6(6).6(6).6(8)]

Cycle sequence ; Size 3 4 5 6

Num 2 2 6 48

Point symbol for net: {3^2.4^2.5^2.6^9} {3^2.4^5.5^5.6^8.7}2

6,7-c net with stoichiometry (6-c)(7-c)2; 2-nodal net

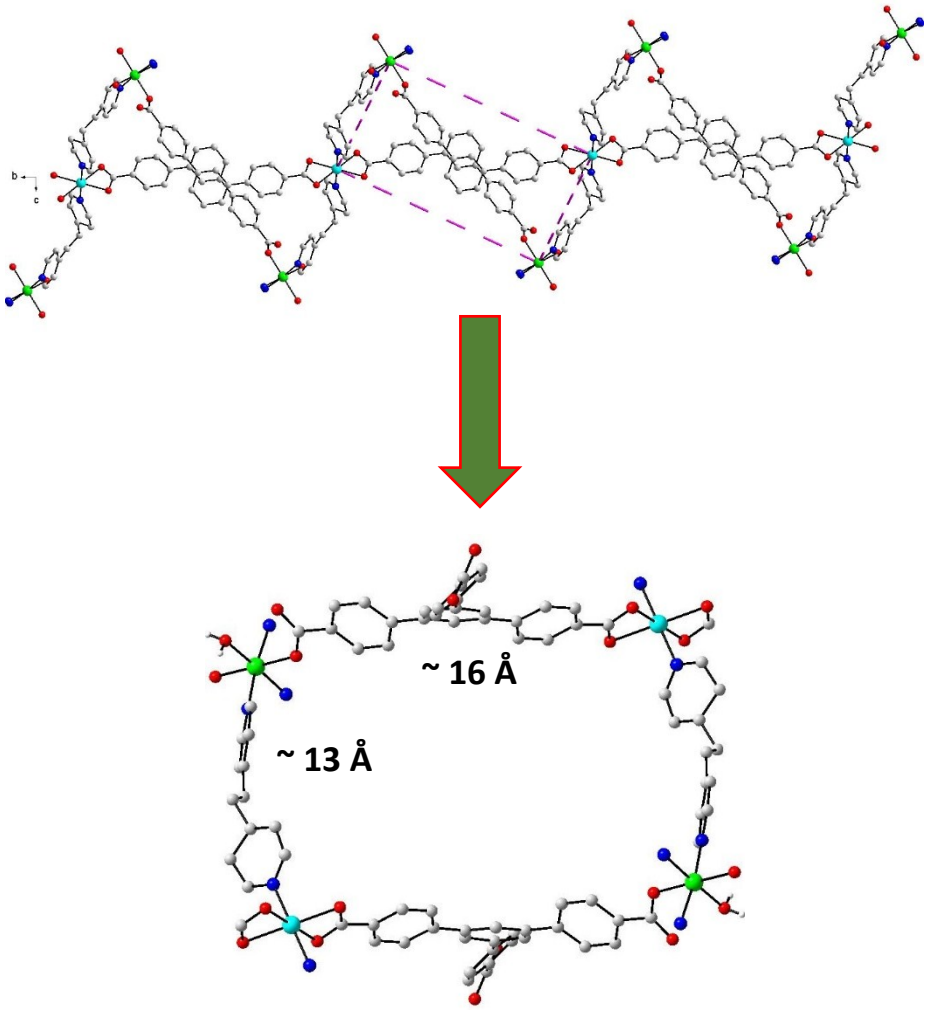

Figure S1. Rectangular ring structure present in compound **1**.

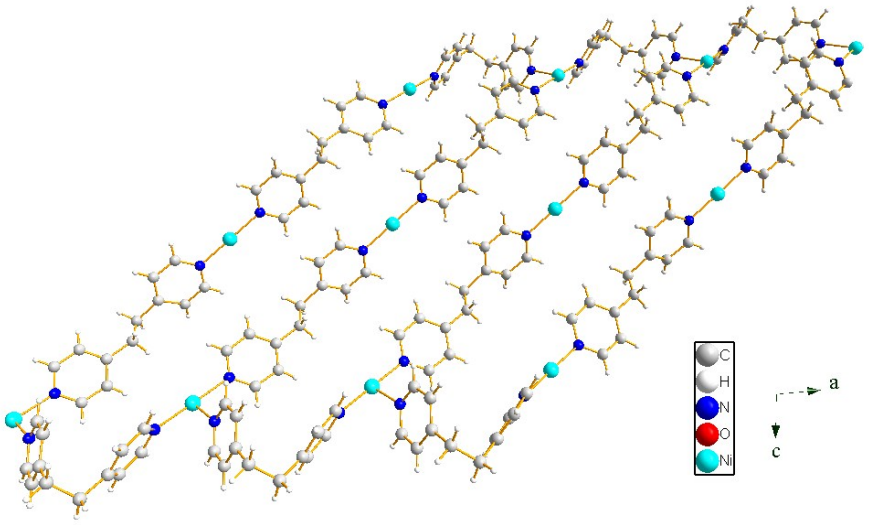

Figure S2. Different modes of BPE connectivity in compound **1**.

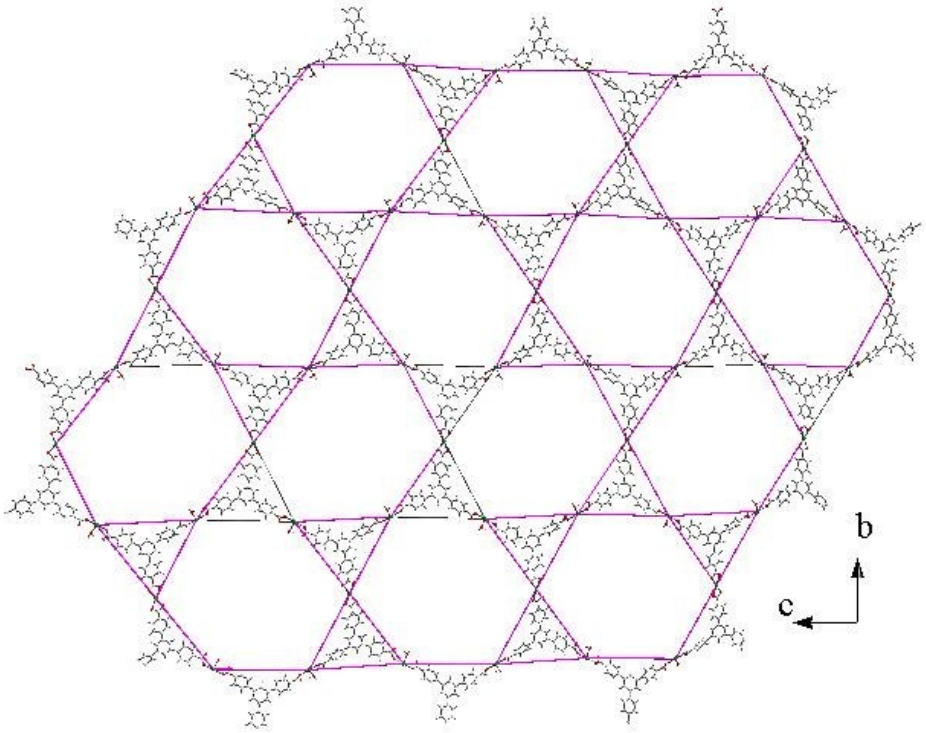

Figure S3. Two-dimensional kagome connectivity between BTB and Ni atoms in a single layer.

Powder X-ray diffraction data:

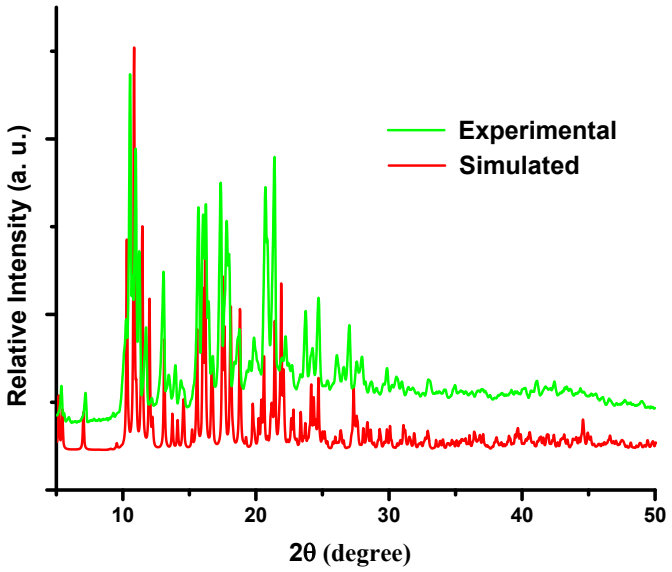

Figure S4a. Experimental and simulated PXRD pattern of compound **1**.

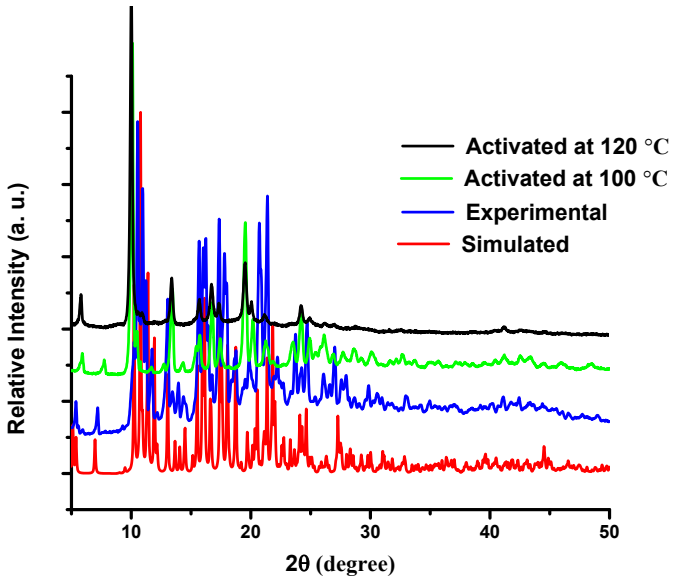

Figure S4 (b) PXRD pattern of compound **1** at different temperatures in vacuum condition

Note: To know the stability of compound **1**, we have activated the sample at different temperatures in vacuum. PXRD pattern clearly confirms that the compound **1** is stable till 100 °C, further heating leads to framework collapse.

Fourier Transform Infrared Spectroscopy (FT-IR) Analysis:

FT-IR of the compound **1** was taken from IR prestige-21 FTIR spectrometer with wavenumber ranging from 500 cm^{-1} to 4000 cm^{-1}. The peaks at the wavenumber 1674 cm^{-1} and 1388 cm^{-1} are due to stretching frequency of C = O (carboxylic acid group) and C = C (aromatic ring) respectively. The broad peak at the wavenumber 2800 - 3600 cm^{-1} is due to -OH stretching band from the coordinated water molecules.

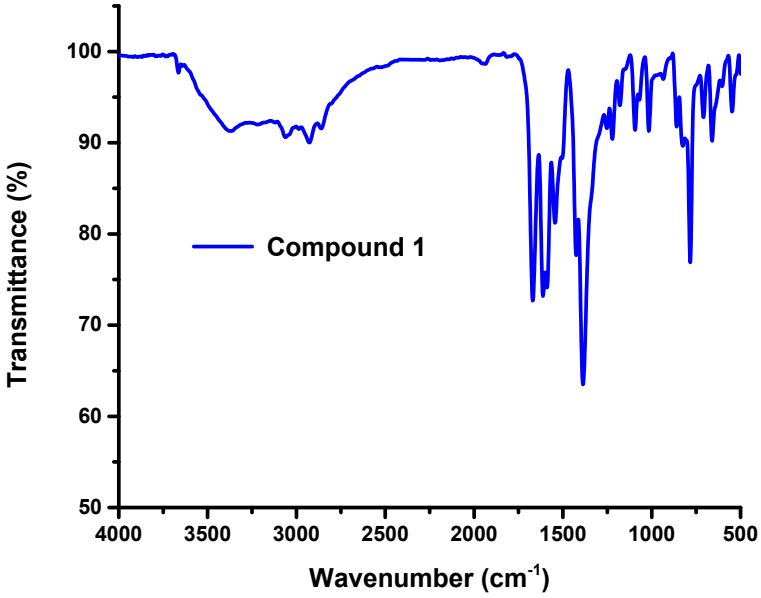

Figure S5. FT-IR spectra for compound **1**.

Thermogravimetric Analysis:

TGA of compound **1** was performed under nitrogen atmosphere in the temperature range from 25 - 900 ^{o}C. TGA graph shows that compound **1** is stable up to 100 ^{0}C.

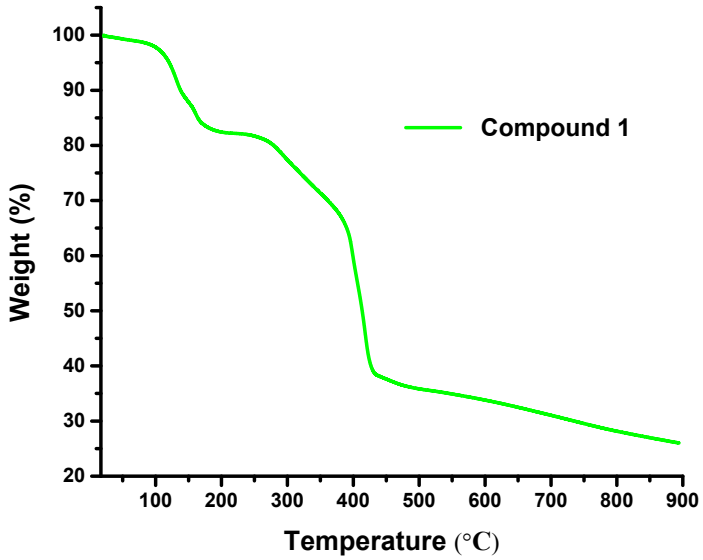

Figure S6. TGA graph for compound **1**.

Gas sorption studies:

Gas sorption measurements were carried out on a Micromeritics' 3Flex gas sorption analyzer. Ultra-high purity N_2 (99.99 %) was used in the sorption experiments. Before gas sorption measurement around 70 mg as synthesized sample was activated at 373 K overnight under dynamic vacuum.

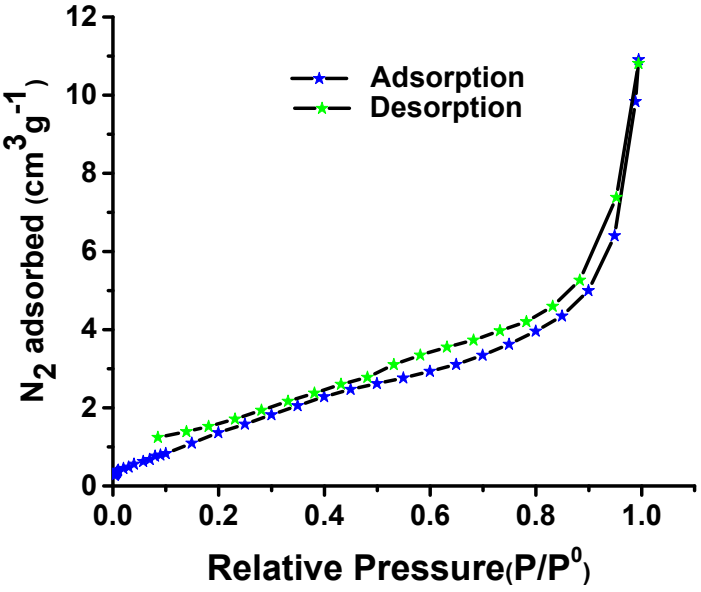

Figure S7. N_2 - adsorption isotherm for compound **1**.

Relevant data for BET fit of the N_2 adsorption isotherm:

BET Surface Area	11.1880 m^2/g
Pore Volume	0.01690 cm^3/g
P/Po	5.1679 m^2/g
Adsorption cumulative surface area	6.442 m^2/g

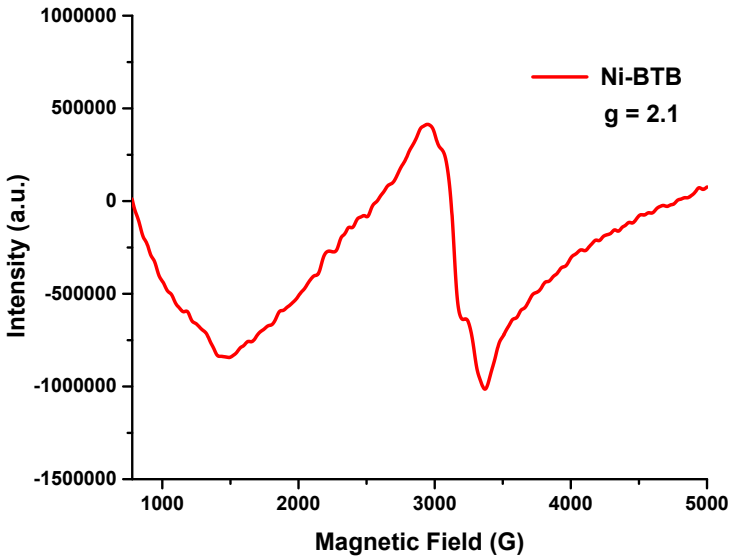

Figure S8. EPR spectrum for compounds **1**.

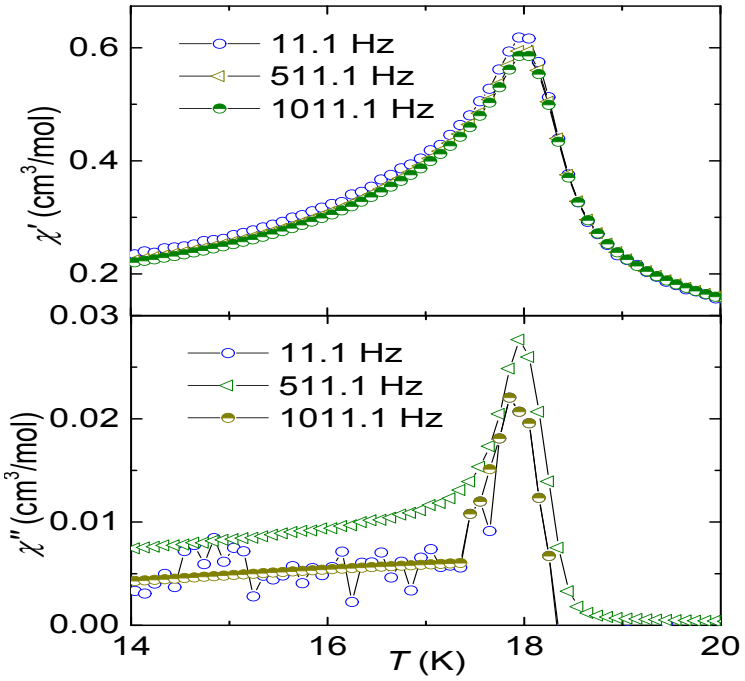

Figure S9. Temperature dependent real (χ') and imaginary (χ") of the AC susceptibility measured at different frequencies.

Band Gap Energy:

The diffuse reflectance spectra of the powder sample of compounds **1** was collected in order to measure the optical band gap energy (E_{bg}). The optical band gap energy was confirmed as the intersection point between the energy axis and the line extrapolated from the linear portion of the absorption edge in a plot of Kubelka-Munk function *vs* energy. Optical band gap energy value is 1.69 eV for compound **1**.

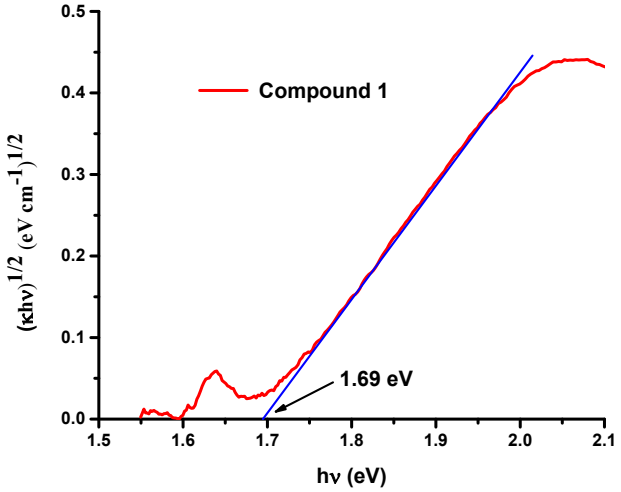

Figure S10. Tauc plots showing the optical-band gap energy for compound **1**.

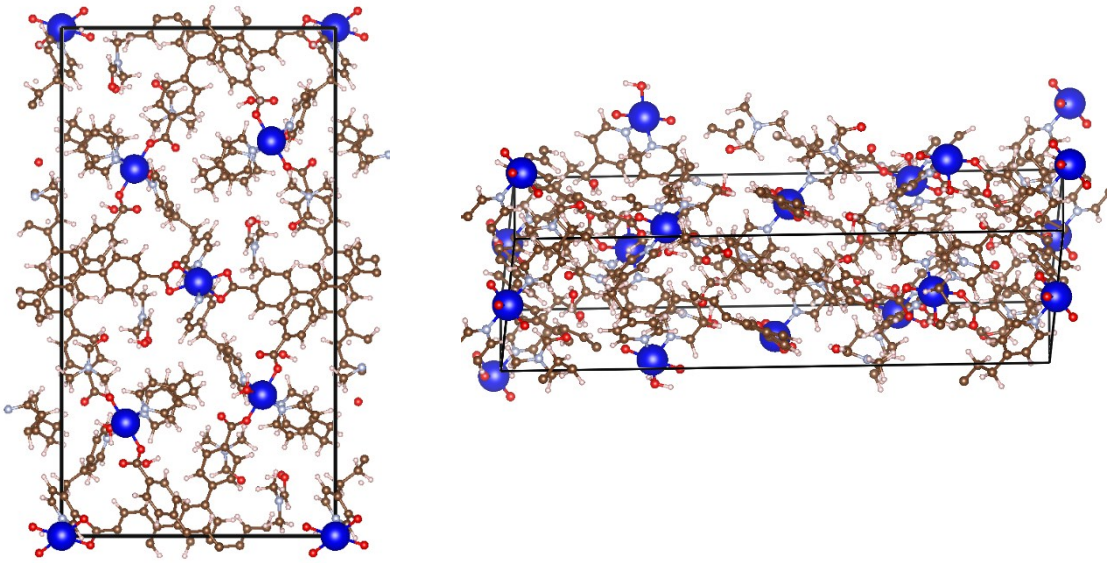

Figure S11. The optimized structures of the compound **1** for the calculation of optical-band gap energy.

Lambda max is at 815 nm =1.52 eV

But there is a small peak at 1252 nm = 0.99 eV (optical gap)

This is calculated from this molecular fragment:

(a)

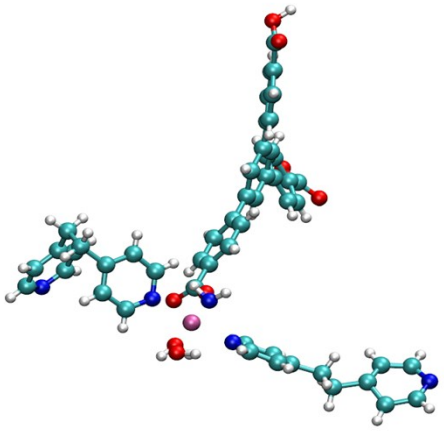

(b)

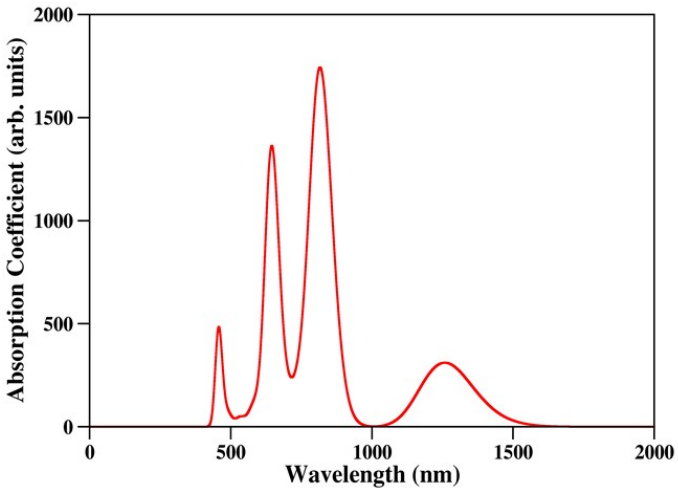

Figure S12. (a) Molecular Fragment, where we calculate the optical absorption spectra theoretically. (b) Theoretically predicted absorption spectra of compound **1**.

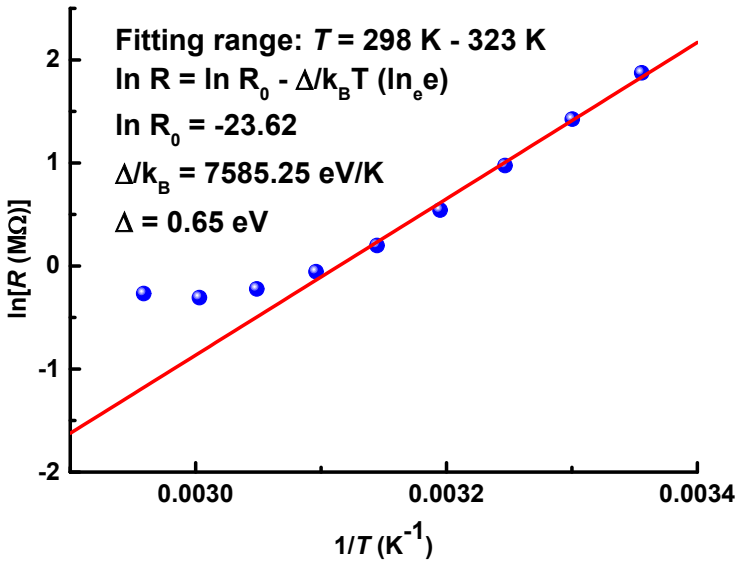

Figure S13. ln R *vs*. 1/T plot. The red straight lines are linear fits to the data between 298 and 323 K.